

Synthesis of cyclohexadiene complexes of (methylidyne)triruthenium clusters. The crystal structure of $(\mu\text{-H})\text{Ru}_3(\mu\text{-}3\text{-COMe})(\text{CO})_8(1,3\text{-C}_6\text{H}_8)$ and a redetermination of the structure of $(\mu\text{-H})\text{Ru}_3(\mu\text{-COMe})(\text{CO})_{10}$

Melvyn Rowen Churchill, Lawrence R. Beanan, Harvey J. Wasserman,
Clifford Bueno, Zuraidah Abdul Rahman, and Jerome B. Keister

Organometallics, 1983, 2 (9), 1179-1186 • DOI: 10.1021/om50003a019 • Publication Date (Web): 01 May 2002

Downloaded from <http://pubs.acs.org> on April 24, 2009

More About This Article

The permalink <http://dx.doi.org/10.1021/om50003a019> provides access to:

- Links to articles and content related to this article
- Copyright permission to reproduce figures and/or text from this article



ACS Publications
High quality. High impact.

Synthesis of Cyclohexadiene Complexes of (Methyldyne)triruthenium Clusters. The Crystal Structure of $(\mu\text{-H})\text{Ru}_3(\mu_3\text{-COCH}_3)(\text{CO})_8(1,3\text{-C}_6\text{H}_8)$ and a Redetermination of the Structure of $(\mu\text{-H})\text{Ru}_3(\mu\text{-COCH}_3)(\text{CO})_{10}$

Melvyn Rowen Churchill,* Lawrence R. Beanan, Harvey J. Wasserman, Clifford Bueno, Zuraidah Abdul Rahman, and Jerome B. Keister*

Department of Chemistry, State University of New York at Buffalo, Buffalo, New York 14214

Received January 17, 1983

The complexes $(\mu\text{-H})\text{Ru}_3(\mu_3\text{-CX})(\text{CO})_8(1,3\text{-cyclohexadiene})$ (1, X = OMe; 2, X = Ph) are formed by reactions of the corresponding $(\mu\text{-H})_3\text{Ru}_3(\mu_3\text{-CX})(\text{CO})_9$ with alkenes in the presence of excess 1,3-cyclohexadiene; 1 equiv of the hydrogenated alkene is also formed. The clusters 1 and 2 have been characterized spectroscopically, and the crystal structure of 1 has been determined by a complete three-dimensional X-ray crystallographic analysis. Because the structure of 1 differs significantly from that of the parent carbonyl $(\mu\text{-H})\text{Ru}_3(\mu\text{-COCH}_3)(\text{CO})_{10}$, a redetermination of the structure of the latter has also been performed. The complex $(\mu\text{-H})\text{Ru}_3(\mu\text{-COCH}_3)(\text{CO})_{10}$ crystallizes in the monoclinic space group $P2_1/c$ with $a = 7.9689$ (17) Å, $b = 17.0158$ (42) Å, $c = 14.1216$ (30) Å, $\beta = 104.082$ (17)°, and $Z = 4$. Diffraction data were collected with a Syntex P2₁ diffractometer and refined to $R_F = 2.6\%$ for all 2444 data with $2\theta(\text{Mo K}\alpha) = 3.5\text{--}45.0^\circ$. The molecule contains a triangular array of ruthenium atoms; four terminal carbonyl ligands are associated with Ru(3), while Ru(1) and Ru(2) are each linked to three. In addition, Ru(1) and Ru(2) are bridged by a hydride ligand and by a $\mu\text{-COCH}_3$ ligand. $(\mu\text{-H})\text{Ru}_3(\mu_3\text{-COCH}_3)(\text{CO})_8(1,3\text{-C}_6\text{H}_8)$ (1) crystallizes in the triclinic space group $P\bar{1}$ with $a = 7.4916$ (17) Å, $b = 8.7077$ (19) Å, $c = 15.6023$ (32) Å, $\alpha = 89.995$ (17)°, $\beta = 97.832$ (17)°, $\gamma = 98.991$ (18)°, and $Z = 2$. Data for $2\theta(\text{Mo K}\alpha) = 4.0\text{--}50.0^\circ$ were collected, and the structure was refined to $R_F = 2.3\%$ for all 3528 reflections. This molecule contains a triangular array of ruthenium atoms capped by a $\mu_3\text{-COCH}_3$ ligand. There are three terminal carbonyl ligands each on Ru(1) and Ru(3), which are bridged by a hydride ligand; Ru(2) is linked to an $\eta^4\text{-1,3-cyclohexadiene}$ ligand and bonded to two carbonyl ligands (which are weakly "semibridging" to Ru(1) and Ru(3)). A comparison of the structures of 1 and those of $(\mu\text{-H})\text{M}_3(\mu\text{-CX})(\text{CO})_{10}$ (M = Fe, Ru, X = O⁻, NMe₂, OMe; M = Os, X = H, NH-*t*-Bu), which have been determined previously, reveals that the coordination geometry adopted by the methyldyne moiety varies in a systematic manner with (i) the metal, (ii) the methyldyne substituent, and (iii) the other ligands of the cluster. These trends may have implications for the geometry adopted by alkyldyne fragments bound to metal surfaces.

Introduction

For a clear understanding of the factors influencing the structures and reactivities of metal carbonyl clusters, systematic studies of the interrelationships between structure, reactivity, metals, and ligands are required. Few such studies have been possible because of the paucity of suitably related cluster series. One series which has been extensively examined is the (methyldyne)tricobalt series $\text{Co}_3(\mu_3\text{-CX})(\text{CO})_9$, where X = alkyl, aryl, halide, and others.¹ The isoelectronic series $(\mu\text{-H})_3\text{M}_3(\mu_3\text{-CX})(\text{CO})_9$, where M = Ru or Os and X = H, Me, Cl, Br, Ph, CO₂Me, or OMe, has only recently been prepared.²⁻⁶ Already the crystal structures of $(\mu\text{-H})_3\text{Ru}_3(\mu_3\text{-CX})(\text{CO})_9$, where X = Me,⁷ CH₂CMe₃,⁸ and Cl,⁹ an infrared analysis¹⁰ for X = H and Cl, and a photoelectron spectroscopic study in conjunction with Fenske-Hall calculations¹¹ have been

reported. We have described some of the chemistry of the methyldyne moiety on the Ru and Os clusters³ and have compared this with the previously reported reactions of the Co analogues.

The presence of hydride ligands in the $(\mu\text{-H})_3\text{M}_3(\mu_3\text{-CX})(\text{CO})_9$ series makes possible studies of hydride reactivity as a function of the metal and the methyldyne substituent. One of us has recently reported on the kinetics and mechanism of reversible reductive elimination of hydrogen from $(\mu\text{-H})_3\text{Ru}_3(\mu_3\text{-COCH}_3)(\text{CO})_9$.¹² In this paper we report the stoichiometric hydrogenation of alkenes by $(\mu\text{-H})_3\text{Ru}_3(\mu_3\text{-CX})(\text{CO})_9$, where X = OMe or Ph, and the subsequent formation of the complexes $(\mu\text{-H})\text{Ru}_3(\mu_3\text{-CX})(\text{CO})_8(1,3\text{-C}_6\text{H}_8)$ when the reaction is conducted in the presence of excess 1,3-cyclohexadiene. Further, the X-ray crystal structure determination for $(\mu\text{-H})\text{Ru}_3(\mu_3\text{-COCH}_3)(\text{CO})_8(1,3\text{-C}_6\text{H}_8)$ is described. Because the structure of the diene complex was unexpectedly found to contain a triply bridging methyldyne, rather than a doubly bridging ligand as in the parent $(\mu\text{-H})\text{Ru}_3(\mu\text{-COCH}_3)(\text{CO})_{10}$,¹³ we have also redetermined the structure of the latter in order to assess as carefully as possible the structural differences between the two clusters.

Experimental Section

Syntheses of $(\mu\text{-H})_3\text{Ru}_3(\mu_3\text{-CX})(\text{CO})_9$, X = OMe⁴ and Ph³, were conducted by using published procedures. Cyclohexadiene was

(1) (a) Seyferth, D. *Adv. Organomet. Chem.* 1976, 14, 97. (b) Penfold, B. R.; Robinson, B. H. *Acc. Chem. Res.* 1973, 6, 73. (c) Pályi, G.; Piacenti, F.; Markó, L. *Inorg. Chim. Acta Rev.* 1970, 4, 109.

(2) Canty, A. J.; Johnson, B. F. G.; Lewis, J.; Norton, J. R. *J. Chem. Soc., Chem. Commun.* 1972, 1331.

(3) Keister, J. B.; Horling, T. L. *Inorg. Chem.* 1980, 19, 2304.

(4) Keister, J. B. *J. Chem. Soc., Chem. Commun.* 1979, 214.

(5) (a) Calvert, R. B.; Shapley, J. R. *J. Am. Chem. Soc.* 1977, 99, 5225.

(b) Azam, K. A.; Deeming, A. J. *J. Chem. Soc., Chem. Commun.* 1977, 472.

(6) Deeming, A. J.; Underhill, M. *J. Chem. Soc., Chem. Commun.* 1973, 277.

(7) Sheldrick, G. M.; Yesinowski, J. P. *J. Chem. Soc., Dalton Trans.* 1975, 873.

(8) Castiglioni, M.; Gervasio, G.; Sappa, E. *Inorg. Chim. Acta* 1981, 49, 217.

(9) Zhu, N. J.; Lecomte, C.; Coppens, P.; Keister, J. B. *Acta Crystallogr., Sect. B* 1982, B38, 1286.

(10) Oxton, I. A., submitted for publication.

(11) Sherwood, D. E., Jr.; Hall, M. B. *Organometallics* 1982, 1, 1519.
(12) Bavaro, L. M.; Montangero, P.; Keister, J. B. submitted for publication in *J. Am. Chem. Soc.*

(13) Johnson, B. F. G.; Lewis, J.; Orpen, A. G.; Raithby, P. R.; Süss, G. *J. Organomet. Chem.* 1979, 173, 187.

purchased from Aldrich and purified before use by passage through an alumina column. IR spectra were recorded on Perkin-Elmer 457 or 467 spectrophotometers and were calibrated with cyclohexane or with polystyrene. NMR spectra were obtained with a Varian EM-390 instrument. Mass spectra were provided by Dr. Robert Minard of the Pennsylvania State University Mass Spectrometry Laboratory. Elemental analyses were provided by Galbraith Laboratories.

Reaction of $(\mu\text{-H})_3\text{Ru}_3(\mu_3\text{-COMe})(\text{CO})_9$ with Diethyl Fumarate. To a solution of the cluster (38 mg, 0.063 mmol) in deuteriochloroform in an NMR tube was added diethyl fumarate (18 mg, 0.10 mmol). After 1 h the ^1H NMR spectrum indicated complete disappearance of $(\mu\text{-H})_3\text{Ru}_3(\mu_3\text{-COMe})(\text{CO})_9$ and conversion of fumarate to succinate. The only cluster product which could be identified in the spectrum was $(\mu\text{-H})\text{Ru}_3(\mu\text{-COMe})(\text{CO})_{10}$ (80% yield by NMR, 75% isolated yield). The yield of diethyl succinate was 0.06 mmol (determined by integration against an internal standard), but only 0.002 mmol of unreacted fumarate was observed in the spectrum.

Reaction of $(\mu\text{-H})_3\text{Ru}_3(\mu_3\text{-COMe})(\text{CO})_9$ with 1,3-Cyclohexadiene. A solution of the cluster (58 mg, 0.096 mmol) and 1,3-cyclohexadiene (55 μL , 0.58 mmol) in deuteriochloroform (0.6 mL) was monitored by ^1H NMR spectroscopy over a 9-day period. The final spectrum indicated the presence of cyclohexene, $(\mu\text{-H})\text{Ru}_3(\mu_3\text{-COMe})(\text{CO})_8(1,3\text{-C}_6\text{H}_8)$, and $(\mu\text{-H})\text{Ru}_3(\mu\text{-COMe})(\text{CO})_{10}$, in addition to unreacted starting materials.

$(\mu\text{-H})\text{Ru}_3(\mu_3\text{-COMe})(\text{CO})_8(1,3\text{-C}_6\text{H}_8)$ (1). Method 1. A solution of $(\mu\text{-H})_3\text{Ru}_3(\mu_3\text{-COMe})(\text{CO})_9$ (100 mg, 0.166 mmol), diethyl fumarate (28 μL , 0.17 mmol), and 1,3-cyclohexadiene (100 μL , 1.0 mmol) in cyclohexane (25 mL) was stirred under nitrogen for 12 h at room temperature. Then the solvent was removed on a rotary evaporator, and the resulting red-orange oil was purified by thin-layer chromatography on silica gel, eluting with cyclohexane. The first band yielded $(\mu\text{-H})\text{Ru}_3(\mu\text{-COMe})(\text{CO})_{10}$ (30 mg, 29%) after extraction with dichloromethane. The second, orange band was 1, isolated as an orange oil (27 mg) after extraction with dichloromethane and removal of solvent. Recrystallization of the oil from methanol gave red crystals (8 mg, 7%).

Method 2. A solution of $(\mu\text{-H})_3\text{Ru}_3(\mu_3\text{-COMe})(\text{CO})_9$ (151 mg, 0.250 mmol) in neat 1,3-cyclohexadiene (15 mL) was stirred under nitrogen and at room temperature for 10 days. Then the solvent was recovered by vacuum transfer, and the red-orange residue (137 mg) was crystallized by cooling to -16°C to give dark red crystals containing ca. 10% $(\mu\text{-H})\text{Ru}_3(\mu\text{-COMe})(\text{CO})_{10}$, as determined by ^1H NMR spectroscopy: IR (C_6H_{12}) 2086 (m), 2066 (vs), 2024 (vs), 2001 (s), 1990 (sh), 1959 (w), 1909 (w) cm^{-1} ; IR (KBr) 2084 (m), 2063 (s, br), 2007 (s, br), 1979 (s), 1933 (m), 1872 (m) cm^{-1} ; ^1H NMR (CDCl_3) τ 4.8 (m, 2 H), 6.15 (s, 3 H), 6.5 (m, 2 H), 8.08 (s, 4 H), 26.39 (s, 1 H); mass spectrum, m/e 627 ($^{101}\text{Ru}_3$) due to decomposition to $(\mu\text{-H})\text{Ru}_3(\mu\text{-COMe})(\text{CO})_{10}$.

$(\mu\text{-H})\text{Ru}_3(\mu_3\text{-CPh})(\text{CO})_8(1,3\text{-C}_6\text{H}_8)$ (2). A solution of $(\mu\text{-H})_3\text{Ru}_3(\mu\text{-CPh})(\text{CO})_9$ (100 mg, 0.15 mmol), 1,3-cyclohexadiene (100 μL , 1.0 mmol), and diethyl fumarate (25 μL , 0.15 mmol) in cyclohexane (25 mL) was stirred under nitrogen and at room temperature for 7 days. The solvent was then removed on a rotary evaporator, and the residue was purified by thin-layer chromatography on silica gel, eluting with cyclohexane. The second, orange-yellow band was extracted with dichloromethane, and then the residue after evaporation was recrystallized from methanol to give dark red crystals (45 mg, 38%): IR (C_6H_{12}) 2090 (m), 2070 (vs), 2033 (vs), 2019 (m), 2008 (m), 2000 (m), 1938 (w), 1883 (w) cm^{-1} ; IR (KBr) 2085 (m), 2067 (s), 2058 (sh), 2019 (s), 2009 (s), 1994 (s), 1925 (m), 1880 (m) cm^{-1} ; ^1H NMR (CDCl_3) τ 2.7 (m, 5 H), 5.2 (m, 2 H), 6.8 (m, 2 H), 8.1 (t, 4 H); mass spectrum, m/e 697 ($^{101}\text{Ru}_3$). Anal. Calcd for $\text{C}_{21}\text{H}_{14}\text{O}_8\text{Ru}_3$: C, 36.16; H, 2.03. Found: C, 36.69; H, 3.02.

X-ray Diffraction Study of $(\mu\text{-H})\text{Ru}_3(\mu_3\text{-COMe})(\text{CO})_8(1,3\text{-C}_6\text{H}_8)$ (1). An opaque, approximately equidimensional red crystal was glued to a glass fiber and mounted in a eucentric goniometer on a Syntex P2₁ automated four-circle diffractometer. The crystal was aligned, and data were collected as described previously;¹⁴ details appear in Table I. All data were converted to $|F_o|$ values following correction for absorption, Lorentz, and

Table I. X-ray Diffraction Data for $(\mu\text{-H})\text{Ru}_3(\mu_3\text{-COMe})(\text{CO})_8(1,3\text{-C}_6\text{H}_8)$ (1) and $(\mu\text{-H})\text{Ru}_3(\mu\text{-COMe})(\text{CO})_{10}$

1		$(\mu\text{-H})\text{Ru}_3(\mu\text{-COMe})(\text{CO})_{10}$
(A) Crystal Parameters at 24 °C		
cryst system:	triclinic	monoclinic
space group	P1 (No. 2)	P2 ₁ /c (No. 14)
a, Å	7.4916 (17)	7.9689 (17)
b, Å	8.7077 (19)	17.0158 (42)
c, Å	15.6023 (32)	14.1216 (30)
α , deg	89.995 (17)	(90)
β , deg	97.832 (17)	104.082 (17)
γ , deg	98.991 (18)	(90)
V, Å ³	995.7 (8)	1857.3 (7)
Z	2	4
mol wt	651.49	627.38
ρ (calcd), g cm ⁻³	2.17	2.24
μ (Mo K α), cm ⁻¹	22.1	24.0
(B) Measurement of Data		
radiation	Mo K α (λ = 0.710 730 Å)	a
monochromator	highly oriented graphite, equatorial mode	a
scan type	coupled θ (crystal)- 2θ (counter)	a
scan speed	3.0 deg/min	a
reflectns measd	+h, $\pm k$, $\pm l$ for 2θ = 4.0-50.0°	+h, $\pm k$, $\pm l$ for 2θ = 3.5-45.0°
no. of independent reflectns	3528	2444
stds	3 every 97 reflections; no significant changes observed	a

^a Entry for $(\mu\text{-H})\text{Ru}_3(\mu\text{-COMe})(\text{CO})_{10}$ identical with that for 1.

polarization factors. Any reflection with $I(\text{net}) < 0$ was assigned a value of $|F_o| = 0$.

All calculations were performed on our in-house NOVA 1200 computer under the SUNY-Buffalo modified version of the Syntex XTL interactive crystallographic program package. The position of the three ruthenium atoms were determined from a Patterson synthesis. The positions of all non-hydrogen atoms and the hydride ligand were determined from a series of difference Fourier calculations. The remaining hydrogen atoms were included in idealized geometry with $d(\text{C-H}) = 0.95$ Å.¹⁵ (Hydrogen atoms of the methyl group centered at C(2) were input assuming a staggered conformation relative to the O(1)-C(1) vector.) Full-matrix least-squares refinement converged smoothly with¹⁶ $R_F = 2.3\%$ and $R_{wF} = 2.6\%$ for 301 variables refined against all 3528 independent reflections ($R_F = 2.0\%$ and $R_{wF} = 2.5\%$ for those 3320 reflections with $|F_o| > 3\sigma(|F_o|)$).

During the calculations the analytical form^{17a} of the scattering factor of the appropriate neutral atom was corrected for both the $\Delta f'$ and $\Delta f''$ components of anomalous dispersion.^{17b} The function minimized during least-squares refinement was $\sum w(|F_o| - |F_c|)^2$ where the weighting scheme is based upon counting statistics, with an "ignorance factor" of 0.03.

Final positional parameters appear in Table II; anisotropic thermal parameters are collected in Table III.

X-ray Diffraction Study of $(\mu\text{-H})\text{Ru}_3(\mu\text{-COMe})(\text{CO})_{10}$. An opaque yellow crystal of approximate dimensions $0.5 \times 0.2 \times 0.1$ mm, prepared as reported previously,⁴ was mounted on our Syntex P2₁ diffractometer, and data were collected as described above (see Table I). The structure had been reported previously,¹³ but

(15) Churchill, M. R. *Inorg. Chem.* 1973, 12, 1213.

(16) $R_F = [\sum w(|F_o| - |F_c|) / \sum |F_o|] \times 100$ (%); $R_{wF} = [\sum w(|F_o| - |F_c|)^2 / \sum w|F_o|^2]^{1/2} \times 100$ (%).

(17) "International Tables for X-Ray Crystallography"; Kynoch Press: Birmingham, England 1974; vol. 4: (a) pp 99-101; (b) pp 149-150.

Table II. Positional Parameters for $(\mu-H)Ru_3(\mu_3-COMe)(CO)_8(1,3-C_6H_8)$

atom	x	y	z	atom	x	y	z
Ru(1)	0.07475 (3)	0.02212 (2)	0.26256 (2)	C(3)	0.2363 (5)	0.4577 (4)	0.0736 (2)
Ru(2)	0.19324 (3)	0.30147 (2)	0.18388 (1)	C(4)	0.3799 (4)	0.4976 (4)	0.1420 (2)
Ru(3)	0.14476 (3)	0.30717 (3)	0.35977 (1)	C(5)	0.4808 (4)	0.3764 (4)	0.1676 (2)
O(1)	0.4808 (3)	0.1743 (3)	0.31121 (14)	C(6)	0.4232 (4)	0.2357 (4)	0.1196 (2)
O(11)	0.1346 (4)	-0.2020 (3)	0.4082 (2)	C(7)	0.3751 (6)	0.2376 (5)	0.0226 (2)
O(12)	-0.3276 (4)	-0.1272 (4)	0.1996 (2)	C(8)	0.2647 (6)	0.3650 (5)	-0.0037 (2)
O(13)	0.2463 (4)	-0.1645 (3)	0.1406 (2)	C(11)	0.1084 (5)	-0.1175 (4)	0.3531 (2)
O(21)	-0.1159 (4)	0.1297 (4)	0.0582 (2)	C(12)	-0.1829 (5)	-0.0698 (4)	0.2212 (2)
O(22)	-0.0513 (4)	0.5351 (3)	0.2154 (2)	C(13)	0.1813 (5)	-0.0965 (4)	0.1864 (2)
O(31)	0.4443 (4)	0.5858 (3)	0.4013 (2)	C(21)	-0.0047 (5)	0.1799 (4)	0.1124 (2)
O(32)	-0.1778 (4)	0.4572 (4)	0.4107 (2)	C(22)	0.0378 (4)	0.4373 (4)	0.2204 (2)
O(33)	0.2290 (4)	0.1610 (3)	0.5338 (2)	C(31)	0.3314 (5)	0.4828 (4)	0.3875 (2)
C(1)	0.3007 (4)	0.1855 (3)	0.2948 (2)	C(32)	-0.0628 (5)	0.4032 (4)	0.3908 (2)
C(2)	0.5376 (6)	0.0788 (7)	0.3784 (4)	C(33)	0.1981 (5)	0.2181 (4)	0.4689 (2)

atom	x	y	z	$B_{iso}, \text{\AA}^2$	atom	x	y	z	$B_{iso}, \text{\AA}^2$
H(1)	-0.036 (4)	0.144 (4)	0.324 (2)	3.6 (7)	H(5)	0.557 (5)	0.391 (4)	0.215 (2)	4.4 (8)
H(2A)	0.478 (10)	-0.041 (9)	0.347 (5)	14.5 (25)	H(6)	0.471 (4)	0.154 (4)	0.139 (2)	3.7 (7)
H(2B)	0.528 (8)	0.121 (7)	0.433 (4)	11.0 (20)	H(7A)	0.316 (7)	0.136 (6)	0.005 (3)	7.8 (13)
H(2C)	0.664 (5)	0.085 (4)	0.378 (2)	4.1 (7)	H(7B)	0.492 (5)	0.250 (4)	0.000 (2)	5.0 (9)
H(3)	0.159 (5)	0.522 (5)	0.066 (3)	5.3 (10)	H(8A)	0.303 (6)	0.441 (5)	-0.045 (3)	6.3 (10)
H(4)	0.406 (4)	0.592 (4)	0.171 (2)	4.0 (8)	H(8B)	0.142 (5)	0.320 (4)	-0.031 (2)	5.3 (9)

Table IV. Positional Parameters for $(\mu-H)Ru_3(\mu-COMe)(CO)_{10}$

atom	x	y	z	atom	x	y	z
Ru(1)	0.32562 (4)	0.05352 (2)	0.16373 (2)	C(4)	0.39438 (52)	0.14898 (24)	0.24545 (29)
Ru(2)	0.15578 (4)	0.19040 (2)	0.20422 (2)	C(5)	0.5711 (11)	0.24627 (43)	0.34497 (66)
Ru(3)	0.14566 (4)	0.05060 (2)	0.31234 (2)	O(11)	0.12729 (46)	-0.09213 (21)	0.06035 (27)
C(11)	0.19465 (54)	-0.03781 (27)	0.09590 (32)	O(12)	0.62152 (52)	-0.04567 (25)	0.27973 (34)
C(12)	0.51249 (62)	-0.00947 (28)	0.23498 (36)	O(13)	0.48242 (43)	0.10007 (20)	-0.00416 (26)
C(13)	0.42686 (51)	0.08239 (25)	0.05852 (34)	O(21)	-0.24211 (52)	0.20171 (22)	0.11848 (39)
C(21)	-0.09824 (71)	0.19597 (29)	0.15031 (42)	O(22)	0.14121 (63)	0.29550 (27)	0.37487 (33)
C(22)	0.14979 (63)	0.25582 (30)	0.31180 (37)	O(23)	0.24578 (73)	0.31831 (26)	0.07629 (35)
C(23)	0.20831 (72)	0.27079 (29)	0.12312 (37)	O(31)	0.19221 (63)	-0.12474 (24)	0.34898 (34)
C(31)	0.17849 (70)	-0.05932 (32)	0.33749 (38)	O(32)	-0.09576 (57)	0.10006 (35)	0.43948 (32)
C(32)	-0.00442 (69)	0.08302 (35)	0.39299 (37)	O(33)	0.47657 (52)	0.08967 (26)	0.47002 (28)
C(33)	0.35599 (67)	0.07742 (28)	0.41118 (36)	O(34)	-0.16501 (43)	0.01425 (23)	0.14070 (26)
C(34)	-0.04799 (62)	0.03006 (27)	0.20271 (36)	O(4)	0.54846 (37)	0.17032 (19)	0.29433 (25)

atom	x	y	z	$B_{iso}, \text{\AA}^2$	atom	x	y	z	$B_{iso}, \text{\AA}^2$
H(1)	0.1435 (54)	0.1170 (26)	0.1210 (32)	5.6 (11)	H(52)	0.521 (12)	0.2415 (58)	0.4099 (69)	16.2 (35)
H(51)	0.680 (10)	0.2474 (49)	0.3596 (60)	12.0 (27)	H(53)	0.5153 (79)	0.2860 (37)	0.3061 (48)	7.8 (19)

we were interested in an unequivocally reliable study with which to compare our C_6H_8 derivative. The previously reported structure (although it had cosmetically pleasing low discrepancy indices of $R_F = 3.1\%$ and $R_{wF} = 3.5\%$ for 2529 data) suffered from some possible inadequacies: (1) It was based upon a set of data collected on a Stoe STADI-2 two-circle diffractometer using uncorrelated $h, 0-20, l$ data. (2) The b axis was determined from diffractometer μ angle measurements (we have determined its value as 17.0158 (42) \AA as compared to the previously reported value of $b = 16.880$ (9) \AA —a change of about 0.8%). (3) The B_{22} values were restrained to $B_{22} = (B_{11} + B_{33})/2$!

The present structure was based on the previously reported positional parameters for all atoms. Full-matrix least-squares refinement led to $R_F = 2.6\%$ and $R_{wF} = 3.1\%$ for 251 variables refined against all 2444 data ($R_F = 2.2\%$ and $R_{wF} = 3.0\%$ for those 2210 data with $|F_o| > 3\sigma(F_o)$). Final positional parameters are given in Table IV; anisotropic thermal parameters are collected in Table V.

Results

Since "insertion" of an alkene into a metal-hydride bond is one of the most important reactions in organometallic chemistry, the reactivity of the $(\mu-H)_3Ru_3(\mu_3-CX)(CO)_9$ cluster series with alkenes was clearly of interest. Diethyl fumarate was stoichiometrically hydrogenated by $(\mu-H)_3Ru_3(\mu_3-COMe)(CO)_9$ in an NMR tube within a 1-h period to yield diethyl succinate (identified by its NMR spectrum); the major metal-containing product was $(\mu-H)Ru_3(\mu-COMe)(CO)_{10}$ (75% isolated yield). Diethyl

maleate reacted in the same manner, but isomerization of maleate to fumarate was observed during the course of the reaction. Nonactivated olefins such as ethylene also reacted with the cluster but more slowly. In no case were intermediates observed by 1H NMR spectroscopy during the reaction, nor were cluster products other than $(\mu-H)Ru_3(\mu-COMe)(CO)_{10}$ observed even when the reaction was conducted in the presence of a large excess of the alkene.

Although monoenes appeared to coordinate too weakly to the triruthenium cluster to form stable products, the cluster species remaining after alkene hydrogenation could be trapped in the presence of 1,3-cyclohexadiene. The reaction of $(\mu-H)_3Ru_3(\mu_3-COMe)(CO)_9$ with 1 equiv of diethyl fumarate and in the presence of 6 equiv of 1,3-cyclohexadiene produced $(\mu-H)Ru_3(\mu_3-COMe)(CO)_8(1,3-C_6H_8)$ (1), in addition to $(\mu-H)Ru_3(\mu-COMe)(CO)_{10}$. The diene complex was also formed, although more slowly, using 1,3-cyclohexadiene alone. The maximum yield of 1 was obtained by using 1,3-cyclohexadiene as solvent. The benzylidyne derivative $(\mu-H)Ru_3(\mu_3-CPh)(CO)_8(1,3-C_6H_8)$ (2) was prepared in the same way, but the reaction required over 1 week to go to completion at room temperature.

The diene complexes 1 and 2 were initially characterized by spectroscopic methods. The mass spectrum of 2 displayed the molecular ion and ions resulting from stepwise loss of eight carbonyls, as well as the C_6H_8 and C_6H_5 moieties. 1 apparently decomposed in the inlet of the mass

spectrometer, yielding $(\mu\text{-H})\text{Ru}_3(\mu\text{-COMe})(\text{CO})_{10}$. The ^1H NMR spectra of 1 and 2 indicated, in each case, the presence of a single bridging hydride ligand (1, τ 26.39 (s); 2, τ 27.1 (s)) and the appropriate methyldiene substituent; the resonances due to the diene were in each case as expected for a coordinated 1,3-diene.¹⁸ The IR spectra of 1 and 2 between 2150 and 1600 cm^{-1} were very similar, implying similar arrangements of carbonyl ligands; bands attributable to semibridging carbonyls were observed (1, 1909 (w) cm^{-1} in C_6H_{12} , 1872 (m) cm^{-1} in KBr; 2, 1883 (w) cm^{-1} in C_6H_{12} , 1880 (m) cm^{-1} in KBr). Although the spectra of both 1 and 2 in cyclohexane solution were shifted to slightly higher frequencies than in the solid state, we attribute this to a matrix effect, rather than differing solution and solid-state structures, because of the close agreement in the numbers and intensities of the bands in the spectra.

Attempts to prepare other complexes $(\mu\text{-H})\text{Ru}_3(\mu_3\text{-COMe})(\text{CO})_8(\text{diene})$ were unsuccessful. From reactions of $(\mu\text{-H})_3\text{Ru}_3(\mu_3\text{-COMe})(\text{CO})_9$ with 1,3-butadiene or 1,5-cyclooctadiene, only $(\mu\text{-H})\text{Ru}_3(\mu\text{-COMe})(\text{CO})_{10}$ could be isolated. In the case of norbornadiene, a polymeric organic material was formed, and no cluster products were observed by infrared spectroscopy.

The formation of 1 and 2 by hydrogenation of an alkene in the presence of a diene is similar to the formation of $\text{Os}_3(\text{CO})_{10}(\text{diene})$ complexes by reaction of $(\mu\text{-H})_2\text{Os}_3(\text{CO})_{10}$ with dienes.¹⁹ However, since $(\mu\text{-H})_3\text{Ru}_3(\mu_3\text{-CX})(\text{CO})_9$ is saturated, unlike the osmium cluster, carbonyl dissociation is required prior to alkene hydrogenation. This presumably accounts for the much slower rate of reaction when $\text{X} = \text{Ph}$ than when $\text{X} = \text{OMe}$; the rate of substitution by triphenylarsine on $(\mu\text{-H})_3\text{Ru}_3(\mu_3\text{-COMe})(\text{CO})_9$ is 20 times faster than that of $(\mu\text{-H})_3\text{Ru}_3(\mu\text{-CPh})(\text{CO})_9$.²⁰ The faster rate of hydrogenation of diethyl fumarate, compared to that of ethylene or cyclohexadiene, is probably due to the differing equilibrium constants for alkene coordination. Mechanistic studies are in progress.

Although the compositions of 1 and 2 had been established, both the location of the cyclohexadiene ligand and the mode of coordination of the methyldiene ligand were uncertain. Therefore, we undertook a single-crystal X-ray structural determination for 1. It was expected that the structure would be derived from that found for $(\mu\text{-H})\text{Ru}_3(\mu\text{-COMe})(\text{CO})_{10}$ ¹³ with the diene occupying two adjacent sites on a single metal atom. Instead, we found a methyldiene bridging nearly symmetrically all three ruthenium atoms. Since the factors influencing the coordination geometry of alkylidyne ligands are poorly understood, we have also re-determined the structure of $(\mu\text{-H})\text{Ru}_3(\mu\text{-COMe})(\text{CO})_{10}$ to more accurately establish the differences between the structures of these molecules and also to compare them to those of the related clusters $(\mu\text{-H})\text{Ru}_3(\mu\text{-CNMe}_2)(\text{CO})_{10}$ ²¹ and $(\mu\text{-H})\text{Ru}_3(\mu\text{-CO})(\text{CO})_{10}$.²²

In considering the molecular geometry of the species $(\mu\text{-H})\text{Ru}_3(\mu_3\text{-COMe})(\text{CO})_8(1,3\text{-C}_6\text{H}_8)$ (1) and $(\mu\text{-H})\text{Ru}_3(\mu\text{-COMe})(\text{CO})_{10}$, it is more convenient to discuss the unsubstituted species first.

Molecular Geometry of $(\mu\text{-H})\text{Ru}_3(\mu\text{-COMe})(\text{CO})_{10}$

(18) For example, for $\text{Os}_3(\text{CO})_{10}(1,3\text{-C}_6\text{H}_8)$: τ 4.44 (m, 2 H), 6.52 (m, 2 H), 8.15 (t, 4 H) at 28 °C.¹⁹

(19) (a) Tachikawa, M.; Shapley, J. R.; Haltiwanger, R. C.; Pierpont, C. G. *J. Am. Chem. Soc.* 1976, 98, 4651. (b) Bryan, E. G.; Johnson, B. F. G.; Kelland, J. W.; Lewis, J.; McPartlin, M. *J. Chem. Soc., Chem. Commun.* 1976, 254.

(20) Abdul Rahman, Z.; Keister, J. B., unpublished results.

(21) Churchill, M. R.; DeBoer, B. G.; Rotella, F. J. *Inorg. Chem.* 1976, 15, 1843.

(22) Johnson, B. F. G.; Lewis, J.; Raithby, P. R.; Süß, G. *J. Chem. Soc., Dalton Trans.* 1979, 1356.

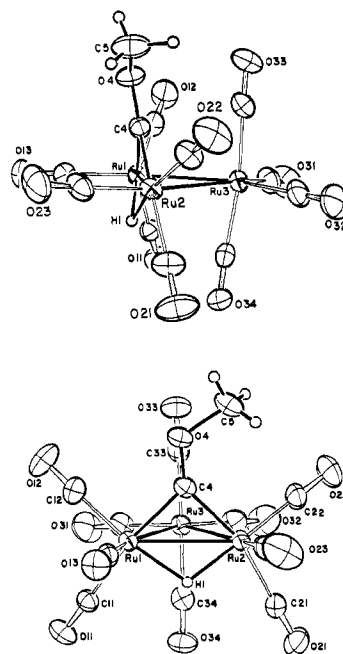


Figure 1. ORTEP-II views (30% ellipsoids, hydrogen atoms artificially reduced) of the $(\mu\text{-H})\text{Ru}_3(\mu\text{-COMe})(\text{CO})_{10}$ molecule.

Table VI. Interatomic Distances (Å) for $(\mu\text{-H})\text{Ru}_3(\mu\text{-COMe})(\text{CO})_{10}$

(A) Ru-Ru and Ru-H Distances			
Ru(1)-Ru(2)	2.821 (0)	Ru(1)-H(1)	1.79 (4)
Ru(1)-Ru(3)	2.816 (0)	Ru(2)-H(1)	1.70 (4)
Ru(2)-Ru(3)	2.838 (0)		
(B) Distances Involving the $\mu\text{-COMe}$ Fragment			
Ru(1)-C(4)	1.991 (4)	C(4)-O(4)	1.305 (5)
Ru(2)-C(4)	1.978 (4)	C(4)-C(5)	1.467 (8)
Ru(3)-C(4)	2.921 (4)		
(C) Distances within Ru-C-O Systems			
Ru(1)-C(11)	1.984 (4)	C(11)-O(11)	1.124 (6)
Ru(1)-C(12)	1.911 (5)	C(12)-O(12)	1.125 (7)
Ru(1)-C(13)	1.919 (4)	C(13)-O(13)	1.123 (6)
Ru(2)-C(21)	1.984 (6)	C(21)-O(21)	1.129 (7)
Ru(2)-C(22)	1.893 (5)	C(22)-O(22)	1.133 (7)
Ru(2)-C(23)	1.895 (5)	C(23)-O(23)	1.130 (7)
Ru(3)-C(31)	1.910 (6)	C(31)-O(31)	1.127 (7)
Ru(3)-C(32)	1.922 (5)	C(32)-O(32)	1.130 (7)
Ru(3)-C(33)	1.956 (5)	C(33)-O(33)	1.126 (7)
Ru(3)-C(34)	1.933 (5)	C(34)-O(34)	1.145 (6)

Two views of the molecule are shown in Figure 1. Interatomic distances and angles are provided in Tables VI and VII. It should be emphasized that most intramolecular measurements are in good agreement with those reported previously by Johnson, Lewis, Orpen, Raithby, and Süß¹³ (hereafter referred to as JLORS). The esd's on our current measurements are, in all cases, substantially lower than those reported by JLORS; furthermore, it is our belief (vide supra) that the (probably minor) systematic errors involved in the JLORS treatment (lack of accuracy in the measurement of the b axis and incorrect treatment of the anisotropic thermal parameters) should be eliminated. The following points may be noted:

(1) The μ -hydrido μ -methoxymethylidyne bridged Ru(1)-Ru(2) distance of 2.821 (0) Å (JLORS 2.803 (2) Å) is no longer distinguishable from the nonbridged distances of Ru(1)-Ru(3) = 2.816 (0) Å and Ru(2)-Ru(3) = 2.838 (0) Å (JLORS 2.810 (2) and 2.821 (2) Å).

(2) The methoxymethylidyne ligand is in a symmetrical μ -bridging mode with Ru(1)-C(4) = 1.991 (4) Å and Ru(2)-C(4) = 1.978 (4) Å (JLORS 1.976 (6) and 1.978 (7) Å);

Table VII. Selected Interatomic Angles (deg) for $(\mu-H)Ru_3(\mu-COMe)(CO)_{10}$

(A) Ru-Ru-Ru, Ru-C-Ru, and Ru-H-Ru Angles			
Ru(3)-Ru(1)-Ru(2)	60.47 (1)	Ru(1)-C(4)-Ru(2)	90.62 (17)
Ru(1)-Ru(2)-Ru(3)	59.67 (1)	Ru(1)-H(1)-Ru(2)	107.7 (23)
Ru(2)-Ru(3)-Ru(1)	59.86 (1)		
(B) Angles within the μ -COMe Fragment			
Ru(1)-C(4)-O(4)	128.64 (31)	C(4)-O(4)-C(5)	119.42 (44)
Ru(2)-C(4)-O(4)	140.33 (32)		
(C) Ru-Ru-(Ligand) Angles			
Ru(2)-Ru(1)-C(4)	44.51 (12)	Ru(3)-Ru(1)-C(4)	72.58 (12)
Ru(2)-Ru(1)-H(1)	35.1 (14)	Ru(3)-Ru(1)-H(1)	75.2 (14)
Ru(2)-Ru(1)-C(11)	121.51 (13)	Ru(3)-Ru(1)-C(11)	92.43 (13)
Ru(2)-Ru(1)-C(12)	135.02 (15)	Ru(3)-Ru(1)-C(12)	94.05 (15)
Ru(2)-Ru(1)-C(13)	104.97 (13)	Ru(3)-Ru(1)-C(13)	165.43 (13)
Ru(1)-Ru(2)-C(4)	44.87 (12)	Ru(3)-Ru(2)-C(4)	72.19 (12)
Ru(1)-Ru(2)-H(1)	37.2 (15)	Ru(3)-Ru(2)-H(1)	75.6 (15)
Ru(1)-Ru(2)-C(21)	117.17 (16)	Ru(3)-Ru(2)-C(21)	94.96 (16)
Ru(1)-Ru(2)-C(22)	139.02 (16)	Ru(3)-Ru(2)-C(22)	92.96 (16)
Ru(1)-Ru(2)-C(23)	106.62 (16)	Ru(3)-Ru(2)-C(23)	165.79 (16)
Ru(1)-Ru(3)-C(31)	94.84 (17)	Ru(2)-Ru(3)-C(31)	154.19 (17)
Ru(1)-Ru(3)-C(32)	160.00 (17)	Ru(2)-Ru(3)-C(32)	100.45 (17)
Ru(1)-Ru(3)-C(33)	91.40 (15)	Ru(2)-Ru(3)-C(33)	93.25 (15)
Ru(1)-Ru(3)-C(34)	81.86 (15)	Ru(2)-Ru(3)-C(34)	80.93 (15)
(D) OC-Ru-CO Angles			
C(11)-Ru(1)-C(12)	93.77 (20)	C(21)-Ru(2)-C(22)	93.58 (22)
C(12)-Ru(1)-C(13)	97.61 (20)	C(22)-Ru(2)-C(23)	96.49 (22)
C(13)-Ru(1)-C(11)	95.61 (18)	C(23)-Ru(2)-C(21)	95.07 (23)
C(31)-Ru(3)-C(32)	104.34 (23)	C(32)-Ru(3)-C(33)	93.37 (22)
C(31)-Ru(3)-C(33)	92.35 (22)	C(32)-Ru(3)-C(34)	92.06 (22)
C(31)-Ru(3)-C(34)	91.06 (22)	C(33)-Ru(3)-C(34)	172.68 (21)
(E) Ru-C-O Angles			
Ru(1)-C(11)-O(11)	176.2 (4)	Ru(2)-C(21)-O(21)	177.6 (5)
Ru(1)-C(12)-O(12)	177.7 (5)	Ru(2)-C(22)-O(22)	178.0 (5)
Ru(1)-C(13)-O(13)	178.3 (4)	Ru(2)-C(23)-O(23)	177.5 (5)
Ru(3)-C(31)-O(31)	177.1 (5)	Ru(3)-C(33)-O(33)	176.9 (5)
Ru(3)-C(32)-O(32)	177.8 (5)	Ru(3)-C(34)-O(34)	176.0 (4)

the metal-carbonyl bond distances trans to these vectors are, unambiguously, the longest in the molecule, with Ru(1)-C(11) = 1.984 (4) Å and Ru(2)-C(21) = 1.984 (6) Å (JLORS 1.989 (7) and 1.987 (8) Å). The next longest are for the mutually trans carbonyls on Ru(3), with Ru(3)-C(33) = 1.956 (5) Å and Ru(3)-C(34) = 1.933 (5) Å (JLORS 1.941 (8) and 1.921 (8) Å). The substituted μ -methylidyne thus exerts a stronger trans influence than does a terminal carbonyl ligand. Other Ru-CO distances lie in the range 1.893 (5)-1.922 (5) Å (JLORS 1.858 (9)-1.915 (9) Å), while C-O distances are 1.123 (6)-1.145 (6) Å (JLORS 1.098 (10)-1.155 (10) Å).

(3) The central atom of the μ -methylidyne ligand is in a planar, trigonal environment with Ru(1)-C(4)-Ru(2) = 90.62 (17)°, Ru(1)-C(4)-O(4) = 128.64 (31)° and Ru(2)-C(4)-O(4) = 140.33 (32)° (JLORS 90.3 (3), 128.9 (5), 140.2 (5)°). The Ru(1)-C(4)-Ru(2) plane makes an angle of 94.90° with the Ru(1)-Ru(2)-Ru(3) plane (see Table VIII).

(4) The C(4)-O(4) distance of 1.305 (5) Å (JLORS 1.299 (8) Å) is clearly indicative of substantial multiple-bond character in this linkage—cf. O(4)-C(5) = 1.467 (8) Å (JLORS 1.427 (9) Å).

(5) All Ru-C-O systems are close-to-linear, with angles in the range 176.0 (4)-178.3 (4)°; there are no indications of semibringing carbonyl ligands.

(6) The axial ligands on Ru(3) are distorted from truly vertical positions with Ru(1)-Ru(3)-C(33) = 91.40 (15)° and Ru(2)-Ru(3)-C(33) = 93.25 (15)° vis à vis Ru(1)-Ru(3)-C(34) = 81.86 (15)° and Ru(2)-Ru(3)-C(34) = 80.93 (15)°. Presumably this results from a combination of (a) repulsion between C(4)-O(4) and the Ru(3)-C(33)-O(33) system and (b) the availability of an appreciable "hole" in

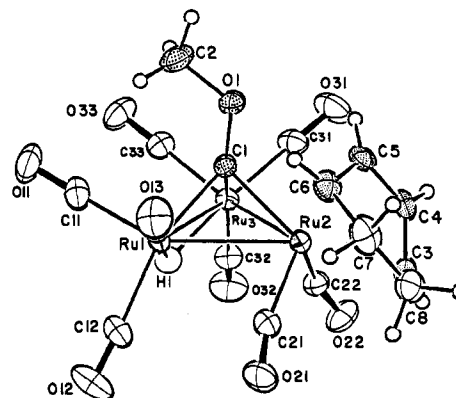


Figure 2. Labeling of atoms in the $(\mu-H)Ru_3(\mu_3-COMe)(CO)_8(1,3-C_6H_8)$ molecule.

the cluster coordination surface lying between the Ru(1)-C(11)-O(11) and Ru(2)-C(21)-O(21) fragments (see Figure 1).

Molecular Geometry of $(\mu-H)Ru_3(\mu_3-COMe)(CO)_8(1,3-C_6H_8)$ (1). This molecule is illustrated in Figure 2. Interatomic distances and angles are collected in Tables IX and X. The most obvious point about this structure is that it is not just related simply to the structure of $(\mu-H)Ru_3(\mu-COMe)(CO)_{10}$ by the replacement of two carbonyl ligands by a 1,3-cyclohexadiene fragment. There have been a number of more significant changes.

(1) The methoxymethylidyne ligand is no longer in a μ -bridging mode. Rather it takes up a slightly distorted μ_3 -bridging (or "capping") mode with Ru(1)-C(1) = 2.039

Table IX. Interatomic Distances (Å) for $(\mu\text{-H})\text{Ru}_3(\mu_3\text{-COMe})(\text{CO})_8(1,3\text{-C}_6\text{H}_8)$ (1)

(A) Ru-Ru and Ru-H Distances			
Ru(1)-Ru(2)	2.799 (0)	Ru(1)-H(1)	1.79 (3)
Ru(1)-Ru(3)	2.848 (0)	Ru(3)-H(1)	1.83 (3)
Ru(2)-Ru(3)	2.818 (0)		
(B) Distances Involving the $\mu_3\text{-COMe}$ Fragment			
Ru(1)-C(1)	2.039 (3)	C(1)-O(1)	1.357 (3)
Ru(2)-C(1)	2.130 (3)	O(1)-C(2)	1.399 (6)
Ru(3)-C(1)	2.055 (3)		
(C) Distances within Ru-C-O Systems			
Ru(1)-C(11)	1.880 (4)	C(11)-O(11)	1.148 (5)
Ru(1)-C(12)	1.990 (4)	C(12)-O(12)	1.127 (5)
Ru(1)-C(13)	1.906 (3)	C(13)-O(13)	1.132 (4)
Ru(2)-C(21)	1.903 (3)	C(21)-O(21)	1.137 (5)
Ru(1)···C(21)	2.758 (3)		
Ru(2)-C(22)	1.921 (3)	C(22)-O(22)	1.158 (4)
Ru(3)···C(22)	2.542 (3)		
Ru(3)-C(31)	1.910 (3)	C(31)-O(31)	1.131 (5)
Ru(3)-C(32)	1.991 (3)	C(32)-O(32)	1.121 (5)
Ru(3)-C(33)	1.890 (3)	C(33)-O(33)	1.139 (4)
(D) Distances Involving the C_6H_8 System			
Ru(2)-C(3)	2.219 (3)	C(3)-C(4)	1.408 (5)
Ru(2)-C(4)	2.191 (3)	C(4)-C(5)	1.419 (5)
Ru(2)-C(5)	2.200 (3)	C(5)-C(6)	1.412 (5)
Ru(2)-C(6)	2.254 (3)	C(6)-C(7)	1.508 (5)
Ru(2)···C(7)	3.110 (4)	C(7)-C(8)	1.509 (6)
Ru(2)···C(8)	3.081 (4)	C(8)-C(3)	1.509 (5)

Table X. Selected Interatomic Angles (Deg) for $(\mu\text{-H})\text{Ru}_3(\mu\text{-COMe})(\text{CO})_8(1,3\text{-C}_6\text{H}_8)$

(A) Ru-Ru-Ru, Ru-C-Ru, and Ru-H-Ru Angles			
Ru(3)-Ru(1)-Ru(2)	59.87 (1)	Ru(1)-C(1)-Ru(2)	84.31 (10)
Ru(1)-Ru(2)-Ru(3)	60.94 (1)	Ru(2)-C(1)-Ru(3)	84.63 (10)
Ru(2)-Ru(3)-Ru(1)	59.19 (1)	Ru(3)-C(1)-Ru(1)	88.17 (11)
Ru(1)-H(1)-Ru(3)	103.6 (15)		
(B) Angles within $\mu_3\text{-COMe}$ Fragment			
Ru(1)-C(1)-O(1)	131.92 (20)	C(1)-O(1)-C(2)	118.20 (29)
Ru(2)-C(1)-O(1)	121.40 (19)		
Ru(3)-C(1)-O(1)	130.35 (20)		
(C) Ru-Ru-(Ligand) Angles			
Ru(2)-Ru(1)-C(1)	49.23 (8)	Ru(3)-Ru(1)-C(1)	46.16 (8)
Ru(2)-Ru(1)-C(11)	146.26 (11)	Ru(3)-Ru(1)-C(11)	99.61 (11)
Ru(2)-Ru(1)-C(12)	114.04 (11)	Ru(3)-Ru(1)-C(12)	118.68 (11)
Ru(2)-Ru(1)-C(13)	92.47 (10)	Ru(3)-Ru(1)-C(13)	141.58 (10)
Ru(1)-Ru(2)-C(1)	46.46 (7)	Ru(3)-Ru(2)-C(1)	46.56 (7)
Ru(1)-Ru(2)-C(3)	155.60 (9)	Ru(3)-Ru(2)-C(3)	141.56 (9)
Ru(1)-Ru(2)-C(4)	159.44 (9)	Ru(3)-Ru(2)-C(4)	115.79 (9)
Ru(1)-Ru(2)-C(5)	122.31 (9)	Ru(3)-Ru(2)-C(5)	111.21 (9)
Ru(1)-Ru(2)-C(6)	100.97 (9)	Ru(3)-Ru(2)-C(6)	130.74 (9)
Ru(1)-Ru(2)-C(21)	68.82 (10)	Ru(3)-Ru(2)-C(21)	113.33 (10)
Ru(1)-Ru(2)-C(22)	102.46 (9)	Ru(3)-Ru(2)-C(22)	61.49 (9)
Ru(1)-Ru(3)-C(1)	45.67 (8)	Ru(2)-Ru(3)-C(1)	48.81 (8)
Ru(1)-Ru(3)-C(31)	140.48 (11)	Ru(2)-Ru(3)-C(31)	93.50 (11)
Ru(1)-Ru(3)-C(32)	119.77 (10)	Ru(2)-Ru(3)-C(32)	117.62 (10)
(D) OC-Ru-CO Angles			
C(11)-Ru(1)-C(12)	95.62 (15)	C(21)-Ru(2)-C(22)	92.21 (14)
C(12)-Ru(1)-C(13)	96.05 (15)	C(31)-Ru(3)-C(32)	97.55 (14)
C(13)-Ru(1)-C(11)	92.26 (15)		
(E) Ru-C-O Angles			
Ru(1)-C(11)-O(11)	177.9 (3)	Ru(2)-C(22)-O(22)	157.7 (3)
Ru(1)-C(12)-O(12)	177.2 (3)	Ru(3)···C(22)-O(22)	125.0 (2)
Ru(1)-C(13)-O(13)	178.7 (3)	Ru(3)-C(31)-O(31)	177.7 (3)
Ru(2)-C(21)-O(21)	166.4 (3)	Ru(3)-C(32)-O(32)	178.1 (3)
Ru(1)···C(21)-O(21)	122.4 (3)	Ru(3)-C(33)-O(33)	178.4 (3)
(F) Angles within C_6H_8 Ligand			
C(8)-C(3)-C(4)	120.2 (3)	C(5)-C(6)-C(7)	120.3 (3)
C(3)-C(4)-C(5)	114.9 (3)	C(6)-C(7)-C(8)	110.9 (3)
C(4)-C(5)-C(6)	114.8 (3)	C(7)-C(8)-C(3)	111.7 (3)

(3) Å, Ru(2)-C(1) = 2.130 (3) Å, and Ru(3)-C(1) = 2.055 (3) Å.

(2) The μ -hydrido-bridged ruthenium-ruthenium bond Ru(1)-Ru(3) = 2.840 (0) Å is demonstrably longer than the bonds Ru(1)-Ru(2) = 2.799 (0) Å and Ru(2)-Ru(3) = 2.818 (0) Å even though all three ruthenium atoms are "capped" by the $\mu_3\text{-COMe}$ ligand.

(3) The carbonyl ligands trans to atom C(1) are still associated with the longest Ru-CO distances (viz., Ru(1)-C(12) = 1.990 (4) Å and Ru(3)-C(32) = 1.991 (3) Å); there is no carbonyl ligand on Ru(2) directly trans to C(1).

(4) The Ru(1)-C(1)-Ru(3) plane makes an angle of 60.70° with the Ru(1)-Ru(2)-Ru(3) plane, as compared to the equivalent angle of 94.90° in the parent compound $(\mu\text{-H})\text{Ru}_3(\mu\text{-COMe})(\text{CO})_{10}$.

(5) The C(1)-O(1) distance of 1.357 (3) Å is rather similar to the O-Me bond length (O(1)-C(2) = 1.399 (6) Å); clearly the environment of the methylidyne carbon atom is now closer to that of a tetrahedral sp^3 -hybridized carbon. Angles (deg) around C(1) are Ru(1)-C(1)-Ru(2) = 84.31 (10), Ru(2)-C(1)-Ru(3) = 84.63 (10), Ru(3)-C(1)-Ru(1) = 88.17 (11), Ru(1)-C(1)-O(1) = 131.92 (20), Ru(2)-C(1)-O(1) = 121.40 (19), and Ru(3)-C(1)-O(1) = 130.35 (20).

(6) Whereas most of the Ru-C-O systems are close to linear (i.e., 177.2 (3)-178.7 (3)°), two are decidedly bent and are involved in "semibridging" carbonyl-dimetal interactions. Thus Ru(2)-C(22)-O(22) = 157.7 (3)° and the Ru(2)-C(22) distance of 1.921 (3) Å is accompanied by a

Ru(3)---C(22) interaction at 2.542 (3) Å, with Ru(3)---C(22)---O(22) = 125.0 (2)°. Similarly, the angle Ru(2)---C(21)---O(21) is 166.4 (3)° and the Ru(2)---C(21) distance of 1.903 (3) Å is associated with a Ru(1)---C(21) interaction at 2.758 (3) Å, with Ru(1)---C(21)---O(21) = 122.4 (3)°. The "α values"²³ for these semibridging carbonyl systems are 0.323 and 0.449, respectively.

The purpose of these semibridging carbonyls is to transfer electron density from the electron-rich atom Ru(2) (19-electron count) to the electron-poor atoms Ru(1) and Ru(3) (17^{1/2} electrons apiece).

The 1,3-Cyclohexadiene Ligand. The 1,3-cyclohexadiene ligand acts as a delocalized four-electron donor, taking up two formal coordination sites on Ru(2). The terminal carbons of the 1,3-diene fragment are slightly more distant than the internal carbon atoms (Ru(2)---C(3) = 2.219 (3) Å and Ru(2)---C(6) = 2.254 (3) Å vs. Ru(2)---C(4) = 2.191 (3) Å and Ru(2)---C(5) = 2.200 (3) Å). Carbon-carbon distances within the 1,3-diene system (C(3)---C(4) = 1.408 (5) Å, C(4)---C(5) = 1.419 (5) Å, C(5)---C(6) = 1.412 (5) Å) are consistent with the accepted model for (cis-1,3-diene) → metal bonding and in good agreement with previously measured values.²⁴⁻²⁸ The ligand is bent across the C(3)---C(6) axis such that there is a dihedral angle of 140.81° (39.19°) between the planar C(3)---C(4)---C(5)---C(6) and C(3)---C(8)---C(7)---C(6) systems (see Table XI).

Discussion

While by no means common, a number of mono- and diene complexes of metal clusters are known, and crystal structures have been determined for several of these. Triruthenium clusters coordinating alkenes have not been previously prepared. Reactions of mono- and dienes with Ru₃(CO)₁₂ or H₄Ru₄(CO)₁₂ give cluster products containing dehydrogenated organic ligands. For example, H₂Ru₃(C-O)₉(C₈H₁₀) is formed from Ru₃(CO)₁₂ and 1,3-cyclooctadiene²⁹ and HRu₃(CO)₉(C₄H₅) from Ru₃(CO)₁₂ and 1,3-butadiene.³⁰

The structure of 1 is unique in that it cannot be regarded as a diene substitution on the parent carbonyl. In contrast, the structure of Os₃(CO)₁₀(*s-cis*-butadiene) is derived from that of Os₃(CO)₁₂ by replacement of one axial and one equatorial carbonyl on a single metal atom by the diene,³¹ and the structure of Co₃(μ₃-CEt)(CO)₇(norbornadiene) is related to that of Co₃(μ₃-CEt)(CO)₉, from which it is prepared, by substitution of two equatorial carbonyls on a single cobalt atom.³² As for Os₃(CO)₁₀(*s-cis*-butadiene), the cyclohexadiene ligand of 1 occupies one axial and one equatorial site on a single metal atom and as for Co₃(μ₃-CEt)(CO)₇(norbornadiene) the diene is coordinated on

the same side of the metal plane as the alkylidyne moiety. However, whereas the osmium and cobalt clusters are electron precise, each metal atom having 18 valence electrons, for 1 the ruthenium atom to which the diene is coordinated has formally 19 electrons, while the other two have only 17^{1/2}; the semibridging carbonyls presumably neutralize this inequality.³³

The question then arises as to why 1 adopts a structure with a triply bridging COMe ligand instead of an electron-precise structure based upon replacement of an axial and an equatorial carbonyl on the unique ruthenium atom of (μ-H)Ru₃(μ-COMe)(CO)₁₀. Structures are now available for the isoelectronic molecules (μ-H)Ru₃(μ-CO)(CO)₁₀,²² (μ-H)Ru₃(μ-CNMe₂)(CO)₁₀,²¹ (μ-H)Ru₃(μ-COMe)(CO)₁₀,¹³ (μ-H)Os₃(μ-CNMe₂)(CO)₁₀,³⁴ (μ-H)Os₃(μ₃-CH)(CO)₁₀,³⁵ (μ-H)Fe₃(μ-CO)(CO)₁₀,³⁶ (μ-H)Fe₃(μ-CNMe₂)(CO)₁₀,³⁷ and (μ-H)Fe₃(μ-COMe)(CO)₁₀,³⁸ as well as 1 reported here. All of these structures contain 12 ligands located at the corners of an icosahedron surrounding a metal triangle.^{39,40} The structures differ primarily in the orientation of the metal triangle within the icosahedral ligand shell.

A comparison of the structures for the clusters listed above reveals systematic changes in the orientation of the M₃ unit as a function of (i) the metal, (ii) the methylidyne substituent, and (iii) other ligands on the cluster. The orientation of the metal triangle with respect to the methylidyne ligand can be indicated by the dihedral angle β between the M₃ plane and the M₂(μ-C) plane. For related clusters differing only in the identity of the metal, the angle β is more acute when the metal is iron than when it is ruthenium. Thus, for (μ-H)M₃(μ-CO)(CO)₁₀ (M = Fe, 102°; M = Ru, 104°), (μ-H)M₃(μ-CNMe₂)(CO)₁₀ (M = Fe, 97°; M = Ru, 100°), and (μ-H)M₃(μ-COMe)(CO)₁₀ (M = Fe, 91°; M = Ru, 95°) in each case the metal triangle is tilted further toward the methylidyne carbon within the icosahedron of 12 ligands when the metal is iron. No strictly comparable osmium clusters have been studied crystallographically, but the fact that the angle β for (μ-H)Os₃(μ-CNMe₂)(CO)₁₀ is 106° may indicate that the trend extends to the third row, as well. The methylidyne substituent exerts an even larger influence upon the structure adopted. For a given metal the angle β for (μ-H)M₃(μ-CX)(CO)₁₀ decreases in the order X = O⁻ > NMe₂ > OMe. For (μ-H)Os₃(μ₃-CH)(CO)₁₀ the methylidyne carbon bridges all three metal atoms, but the distance from carbon to the unique osmium atom is longer than the other two (2.353 (10) Å vs. 2.011 (12) Å); thus, the angle β is much smaller when X = H than when X = NH-*t*-Bu. Finally, a comparison of 1 and (μ-H)Ru₃(μ-COMe)(CO)₁₀ indicates that for a given metal and a given methylidyne substituent the other ligands exert an even larger influence

(23) Curtis, M. D.; Han, K. R.; Butler, W. H. *Inorg. Chem.* 1980, 19, 2096.

(24) Co(η⁵-C₅H₅)(η⁴-1,3-C₂H₄): (a) Churchill, M. R.; Mason, R. *Proc. Chem. Soc., London* 1963, 112. (b) Churchill, M. R.; Mason, R. *Proc. R. Soc., London, Ser. A* 1964, 279, 191.

(25) Fe(η⁴-1,3-C₆F₃)(CO)₅: (a) Churchill, M. R.; Mason, R. *Proc. Chem. Soc., London* 1964, 226. (b) Churchill, M. R.; Mason, R. *Proc. R. Soc., London, Ser. A* 1967, 301, 433.

(26) Rh(η⁵-C₅H₅)(η⁴-1,3-C₆(CF₃)₃): (a) Churchill, M. R.; Mason, R. *Proc. Chem. Soc., London* 1963, 365. (b) Churchill, M. R.; Mason, R. *Proc. R. Soc., London, Ser. A* 1966, 292, 61.

(27) Churchill, M. R.; Mason, R. *Adv. Organomet. Chem.* 1967, 5, 93-135. (See, Specially, pp 100-105.)

(28) Churchill, M. R.; Bird, P. H. *Inorg. Chem.* 1969, 8, 1941. (See, especially, Table VIII on p 1948.)

(29) Canty, A. J.; Domingos, A. J. P.; Johnson, B. F. G.; Lewis, J. J. *Chem. Soc., Dalton Trans.* 1973, 2056.

(30) Gambino, O.; Valle, M.; Aime, Sr.; Vaglio, G. A. *Inorg. Chim. Acta* 1974, 8, 71.

(31) Pierpont, C. G. *Inorg. Chem.* 1978, 17, 1976.

(32) Ng, Y. S.; Penfold, B. R. *Acta Crystallogr., Sect. B* 1978, B34, 1978.

(33) Cotton, F. A.; Troup, J. M. *J. Am. Chem. Soc.* 1974, 96, 1233.

(34) Adams, R. D.; Golembeski, N. M. *Inorg. Chem.* 1979, 18, 2255.

(35) Shapley, J. R.; Cree-Uchiyama, M. E.; St. George, G. M.; Churchill, M. R.; Bueno, C. J. *Am. Chem. Soc.*, 1983, 105, 140.

(36) Dahl, L. F.; Blount, J. F. *Inorg. Chem.* 1965, 4, 1373.

(37) Herbstein, F. H. *Acta Crystallogr., Sect. B* 1981, B37, 339.

(38) Shriver, D. F.; Lehman, D.; Strobe, D. *J. Am. Chem. Soc.* 1975, 97, 1594.

(39) Johnson has recently proposed that intra- and intermolecular packing forces play a major role in determining the ligand arrangements for metal carbonyl clusters.⁴⁰ For the case of twelve ligands surrounding a trimetal core, two possibilities were considered—the icosahedron (as for Fe₃(CO)₁₂) and the anticuboctahedron (as for Ru₃(CO)₁₂). Since all of the structures discussed here are described by the icosahedral arrangement, we have not attempted to relate these structures according to Johnson's proposal. However, it should be noted that the sums of all distances between adjacent ligands defining the icosahedron for 1 and for (μ-H)Ru₃(μ-COMe)(CO)₁₀ differ by less than 10%.

(40) (a) Benfield, R. E.; Johnson, B. F. G. *J. Chem. Soc., Dalton Trans.* 1980, 1743. (b) Johnson, B. F. G. *J. Chem. Soc., Chem. Commun.* 1976, 211.

upon the coordination geometry adopted by the methylidyne ligand, enough to determine whether the group will be doubly or triply bridging.

A comparison of the related molecules $(\mu\text{-H})\text{M}_3(\mu\text{-CX})(\text{CO})_{10}$ where X = O⁻, NMe₂, and OMe indicates that the structural trend cannot be due to the steric bulk of the CX moiety; rather, as the electronegativity of X increases, the angle β decreases. In effect, as the methylidyne carbon moves toward the unique metal atom (decreasing β) the degree of C-X multiple bonding decreases and the degree of M-C bonding increases. This can be shown by comparisons of the C-X bond distances^{4,13,21} and stretching frequencies^{4,13,22,41} and by the barrier to rotation about the C-OMe and C-NR₂ bonds.⁴² Thus, the substituent effect may be explained as a competition between C-X π bonding, for which the doubly bridging geometry is most favorable, and M-C bonding, for which a triply bridging geometry is most favorable.

The explanations for the effects of the metal and the other ligands upon the coordination mode of the methylidyne ligand cannot be made at this time because of the small number of suitably related examples. A dramatic effect is observed upon replacing two carbonyls of $(\mu\text{-H})\text{Ru}_3(\mu\text{-COMe})(\text{CO})_{10}$ by cyclohexadiene, but since this ligand differs from two carbonyls in both size and electronic properties, further examples of ligand effects upon the methylidyne coordination are needed to define the trend.

(41) Gavens, P. D.; Mays, M. J. *J. Organomet. Chem.* **1978**, *162*, 389.

(42) ¹H and ¹³C NMR studies of HO₃($\mu\text{-COR}$)(CO)₁₀ (R = Me⁴¹ or Et⁴⁴) found the free energy of activation for rotation about the C-OR bond to be ca. 13.5 kcal, while that for the C-NR₂ bond of HO₃($\mu\text{-CN}(\text{Me})\text{CH}_2\text{Ph}$)(CO)₁₀, which is static on the NMR time scale, must be greater than 20 kcal/mol.⁴³

(43) Keister, J. B., unpublished results.

The environmental effects on methylidyne coordination discussed here may be of significance to other situations, as well. Studies of hydrocarbons chemisorbed on metal surfaces have implicated methylidyne radicals. An EELS study of acetylene adsorbed on a Ni(111) crystal surface provided evidence for an unsymmetrically bridging CH fragment,⁴⁴ whereas a symmetrically bridging CMe unit has been proposed for ethylene chemisorbed on Pt(111).⁴⁵ Our results suggest that the bonding mode adopted by such a fragment on the surface may be dependent upon the metal, the substituent on the methylidyne, and the other molecules on the surface. Further study of metal clusters should provide both model compounds for spectroscopic comparison with surface species and information about the factors influencing the bonding.

Acknowledgment. This work was supported by the National Science Foundation through Grants CHE80-23448 (M.R.C.) and CHE81-21059 (J.B.K.) and by the donors of the Petroleum Research Fund, administered by the American Chemical Society (J.B.K.).

Registry No. 1, 86120-32-3; 2, 86120-33-4; $(\mu\text{-H})_3\text{Ru}_3(\mu_3\text{-COMe})(\text{CO})_9$, 71562-47-5; $(\mu\text{-H})\text{Ru}_3(\mu\text{-COMe})(\text{CO})_{10}$, 71737-42-3; $(\mu\text{-H})_3\text{Ru}_3(\mu\text{-CPh})(\text{CO})_9$, 73746-99-3; Ru, 7440-18-8; diethyl fumarate, 623-91-6; diethyl succinate, 123-25-1; 1,3-cyclohexadiene, 592-57-4; 1,3-butadiene, 106-99-0; 1,5-cyanoctadiene, 111-78-4; norbornadiene, 121-46-0.

Supplementary Material Available: Anisotropic thermal parameters (Tables III and V), planes within the molecules (Tables VIII and XI), and list of observed and calculated structure factor amplitudes (Tables XII and XIII) for each molecule (40 pages). Ordering information is given on any current masthead page.

(44) Demuth, J. E.; Ibach, H. *Surf. Sci.* **1978**, *78*, L238.

(45) (a) Ibach, H.; Hopster, H.; Sexton, B. *Appl. Surf. Sci.* **1977**, *1*, 1.
(b) Ibach, H.; Lehwald, S. *J. Vac. Sci. Tech.* **1978**, *15*, 407.